CHEMISTRY & CHEMICAL TECHNOLOGY

Vol. 2, No. 2, 2008 Chemistry

Ragini Raj Singh[1], Amit Ron[1], Nick Fishelson[1], Irena Shur[2], Rina Socher[2], Dafna Benayahu[2] and Yosi Shacham–Diamand[1]

BIOLOGICAL CELL-BASED SCREENING FOR SPECIFIC MEMBRANAL AND CYTOPLASMATIC MARKERS USING DIELECTRIC SPECTROSCOPY

[1] *Department of Electrical Engineering, Faculty of Engineering, Tel-Aviv University, Israel.*
[2] *Department of Cell and Developmental Biology, Sackler Faculty of Medicine, Tel-Aviv University, Israel, ragini@eng.tau.ac.il*

Received: March 31, 2008

Abstract. Dielectric spectroscopy (DS) of living biological cells is based on the analysis of cells suspended in a physiological medium. It provides knowledge of the polarization-relaxation response of the cells to external electric field as function of the excitation frequency. This response is strongly affected by both structural and molecular properties of the cells and, therefore, can reveal rare insights into cell physiology and behaviour. This study demonstrates the mapping potential of DS after cytoplasmic and membranal markers for cell-based screening analysis. The effect of membrane permittivity and cytoplasm conductivity was examined using tagged *MBA* and *MDCK* cell lines respectively. The comparison of the dielectric spectra of tagged and native cell lines reveals clear differences between the cells. In addition, the differences in the matching dielectric properties of the cells were discovered. Those findings support the high distinction resolution and sensitivity of DS after fine molecular and cellular changes, and hence, highlight the high potential of DS as non invasive screening tool in cell biology research.

Keywords: dielectric spectroscopy, interfacial polarization, cell screening, lectin, SEC13.

1. Introduction

Dielectric properties can provide a rare insight into the cellular and molecular state of biological cells. Dielectric study of biological cells was explored for the first time by Hoeber, who investigated the dielectric properties of *Erythrocytes* [1]. The foundations of understanding the dispersion mechanism of biological cells suspended in physiological medium have been suggested by Schwan based on the theories of mixed dielectrics, developed by *Maxwell & Wagner* [2-4]. Since then, the dielectric properties of many cell types have been explored by a number of authors [5-9].

Dielectric properties of biological cells are mainly characterized by β dispersion mechanism which accounts for the medium (MF) and high (HF) range of the radio spectrum [9-10]. This mechanism is due to *Maxwell-Wagner* effect (interfacial polarization, according to Onsager it can also be assumed as molecular polarization [11]) at the external and internal interfaces of the phospholipids membrane [12-14]. In addition, a minor contribution may be due to dispersion of small intracellular organelles, which usually appear as a small adjunct to the β dispersion at high frequencies.

Dielectric spectroscopy (DS) techniques can provide comprehensive knowledge about cell structure and properties, intracellular content, membrane shape and selectivity and many more [15-22]. Dynamic dielectric spectroscopy allows real time quantification of cellular and molecular processes occurring in cells during variety of biological mechanisms like: growth, activity, division *etc.* [23-27].

Recent interests in the development of new throughput, non destructive screening techniques are largely driven by the potential for associating physical methods with cell and molecular biology methodologies. Cell based screening is a powerful method that uses living cells to test the effect of different molecules like drugs and toxicants on the cellular and molecular phenotype of cells. This technique requires the use of high sensitive tools that permit high speed systematic identification of biochemical targets and markers on given cell libraries. This study is aiming to demonstrate the use of DS as potential screening tool for Bio-markers in cell based screening analysis. In order to understand its methodological impact, it is critical to get an insight into more fundamental research of membranal and cytoplasmatic tagging effect.

In this study, *Madin-Darby Canine Kidney Epithelial* (*MDCK*) and *Bone Marrow derived Pre-Osteoblastic* (*MBA*) cell lines have been used to investigate the effectiveness of DS after intracellular and membranal markers respectively. Here the intracellular effect was checked using *SEC13* over-expressing *MDCK* cells. The effect of the membrane was tested by coating *MBA* cells with free *lectin* antibodies that bind glycosylate elements on cell surface. The analyzed dielectric spectra confirm the influence of both markers on the dielectric parameters of the cells. Cytoplasm conductivity of *SEC13* mutants and membrane permittivity of *MBA* coated cells were found to be affected when compared to the native

cell lines. Those findings provide the necessary knowledge regarding the ability to correlate molecular and cellular markers, and changes on the matching complex dielectric spectra and parameters of the cells.

2. Modeling the Dielectric Response of Cells

Analysis of dielectric parameters depends upon cell topography; therefore, an appropriate electric model should be applied based on those characteristics. Most biological cells can be treated as thin insulating shelled component (membrane) enclosing conducting medium (cytoplasm). This simple description brought many theories and models developed by several authors. The first model of shelled-spheroid was introduced by Frick [28], later it was extended to the case of shelled-ellipsoid particles [29]. Those models however, were limited to low frequencies analysis. Since then, several models were proposed by Pauly [30], Hanai [31], and Redwood [32]. Those however, suffered from several limitations. The first complete model was introduced by Asami and Hanai, who for the first time presented unlimited approach for dielectric analysis of suspended shelled ellipsoids [33].

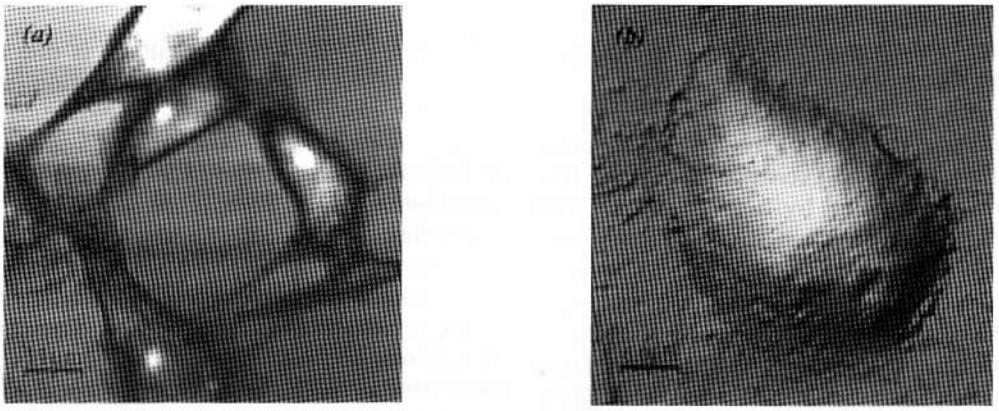

Fig. 1. Topographic images of cells: topography of joined ***MBA*** cells (70×70 mm) (a); topography of single ***MDCK*** cell (40×40 mm) (b). Both images recorded in physiological conditions in DMEM solution

Both *MBA* and *MDCK* cells exhibit approximated elliptic structure (Fig. 1), and therefore, can be treated using the dispersed shelled ellipsoids analysis. Here the cells are described as two phase systems (membrane and cytoplasm) surrounded by infinite and continuous medium (Fig. 2). Based on the theory of interfacial polarization, the complex permittivity of dispersed shelled ellipsoids ε^*, suspended in a medium with complex permittivity ε_m^*, is given by:

$$\varepsilon^* = \varepsilon_m^* + \frac{\Phi}{3}\sum_{k=x,y,z}\frac{\bar{\varepsilon}_m^*\left(\varepsilon_{ck}^* - \varepsilon_m^*\right)}{\bar{\varepsilon}_m^* + \left(\varepsilon_{ck}^* - \bar{\varepsilon}_m^*\right)L_k} \tag{1}$$

where ε_{ck}^* is the complex permittivity of the shelled ellipsoid across the k axis, when:

$$\varepsilon_{ck}^* = \varepsilon_{om}^*\left(1 + \frac{v\left(\varepsilon_i^* - \varepsilon_{om}^*\right)}{\varepsilon_{om}^* + \left(\varepsilon_i^* - \varepsilon_{om}^*\right)L_{ik} - \left(\varepsilon_i^* - \varepsilon_{om}^*\right)vL_k}\right) \tag{2}$$

and v is the volume ratio given by:

$$v = \frac{R_{ix}\cdot R_{iy}\cdot R_{iz}}{\left(R_{ix}+\Delta_L\right)\left(R_{iy}+\Delta_L\right)\left(R_{iz}+\Delta_L\right)} \tag{3}$$

$\Phi = \dfrac{4\pi R_x R_y R_z N}{3}$ is the volume fraction of the cells, Δ_L is membrane thickness and $L_k, L_{ik}\,(k = x,y,z)$ are the depolarization factors, given by:

$$L_{ik} = \frac{R_{ix}R_{iy}R_{iz}}{2}\int_0^\infty \frac{ds}{\left(R_{ik}^2+s\right)\sqrt{\left(R_{ix}^2+s\right)\left(R_{iy}^2+s\right)\left(R_{iz}^2+s\right)}} \tag{4}$$

$$L_k = \frac{R_x R_y R_z}{2}\int_0^\infty \frac{ds}{\left(R_k^2+s\right)\sqrt{\left(R_x^2+s\right)\left(R_y^2+s\right)\left(R_z^2+s\right)}} \tag{5}$$

Here the complex medium permittivity is represented by the average value $\bar{\varepsilon}_m^*$. It can be found within the range of $\varepsilon_m^* \le \bar{\varepsilon}_m^* \le \varepsilon^*$, when it depends on cells concentration. At low concentration, the medium around each cell is assumed to be homogenous (cell free), and therefore, $\bar{\varepsilon}_m^* = \varepsilon_m^*$. When the cells concentration is high, each single cell surrounded by a mixture of cells and medium, and therefore, $\bar{\varepsilon}_m^* \approx \varepsilon^*$.

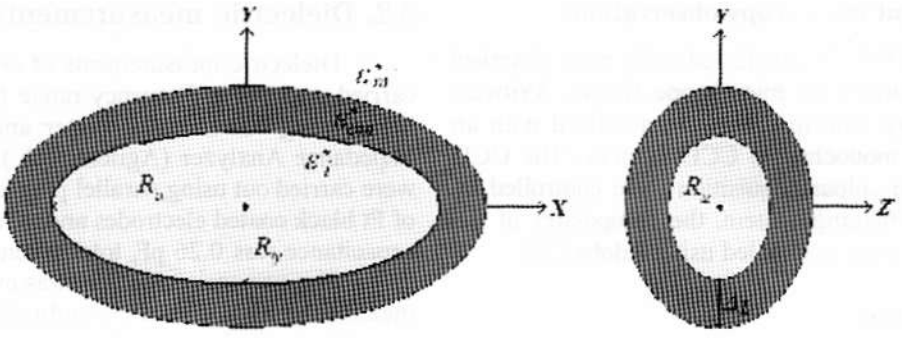

Fig. 2. Shelled ellipsoid model: X–Y plane (left), Y–Z plane (right). ε_m^*, ε_{om}^*, ε_i^* represent the complex permittivity of medium, membrane (red) and cytoplasm (yellow), respectively

3. Experimental

3.1 Preparation and analysis of cells

3.1.1. Cell cultures

Madin-Darby Canine Kidney Epithelial (*MDCK*) wild type or stable transfected with *SEC13*-GFP. *MBA-15* cells are marrow stroma derived osteoprogenitors [34]. The cells were cultured in growth medium Dulbecco's Modified Essential Medium (DMEM) supplemented with 10 % heat-inactivated fetal calf serum (FCS), 1 % glutamine and 1 % antibiotics, and maintained in 5 % CO_2 at 310 K.

3.1.2. Fluorescence-activated cell sorter (FACS)

Binding of *biotinylated-lectin Helix pomatia* (*HPA*, Sigma) to cell surface carbohydrate residues expression were analyzed by FACS. For the analysis adherent cells were released from culture using 0.5 mM EDTA in PBS. Single cell suspensions were blocking buffer, PBS containing 1 % FCS, then the cells were incubated for 30 min on ice with *HPA-biotin* conjugate and stained with Extravidine-FITC (Sigma). 10^4 cells were collected by FACS, and statistical analysis was performed using software from Becton Dickinson as described earlier [35].

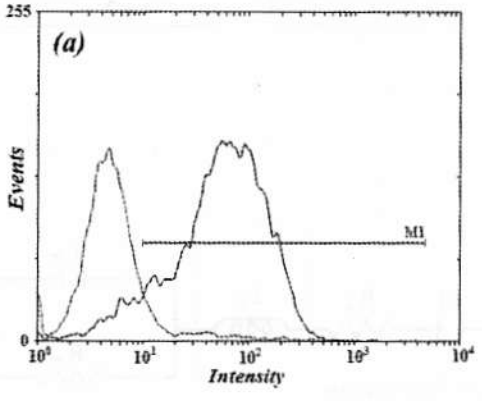

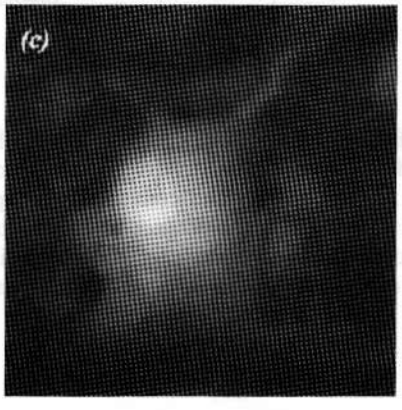

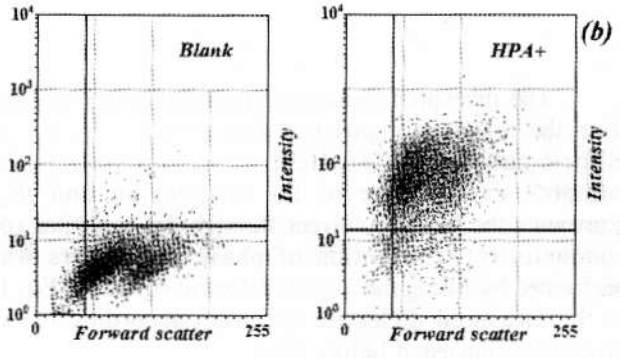

Fig. 3. FACS and GFP analysis
Quantifying FACS data (a): the level of fluorescence intensity is given by the X axis, the number of cells is given by the Y axis. Dot plots of lectin coated cells (*HPA+*) and untagged cells (*blank*) (b): the level of fluorescence intensity is given by the Y axis, the relative size of the cells is represented by the forward scatter signal given by the X axis. Single cell GFP staining of ***sec13*** proteins (c)

3.1.3. Fluorescent microscopy observations

The *MDCK*-GFP-transfected cells were observed with inverted fluorescent microscope (Zeiss, Axiovert 200M, Germany). The images were acquired with an Axiocam MRm monochrome CCD camera. The CCD camera drive and colour acquisition were controlled by Axiovision 4.4 imaging system, the composites of the digitized images were assembled using Adobe [36].

3.1.4 AFM analysis

The morphological parameters of the cells were measured using Atomic Force Microscopy (Pico SPM II, Molecular Imaging). The topography of the cells was recorded in contact mode using Silicon nitride tips (Veeco NP-series, k=0.06 N/m). Force setpoint was taken to be 5 nN with scan rate of 0.4 lines/s. The cells were imaged in physiological conditions in a specific fluid cell covered with 200 µl of the cell serum (growth medium). Several cells were then analyzed in order to obtain their average geometrical dimensions.

3.2. Dielectric measurements

Dielectric measurements of cell suspensions were carried out over a frequency range from 100 Hz to 100 MHz using 4284A LCR meter and 4294A Precision Impedance Analyzer (Agilent tech.). All measurements were carried out using parallel plate condenser consisting of Pt black coated electrodes and a Teflon spacer. The air capacitance was 0.26 pF, total volume of 750 µl.

The suspension medium was evaluated before each measurement for both conductivity and relative permittivity. Cells at specific concentration were filtered out from the growth medium and then suspended again in a fresh medium (total volume of 750 µl) before each measurement. All measurements were performed at room temperature (298 K); evolution of measurements is summarized in Table 1. The measured data was corrected for leads/cell inductance and polarization impedance (section 3.3). In addition, non linearity of current was checked to avoid errors in correction of polarization impedance which can have large impact on the measured data (section 3.3).

Table 1

Measurements of cell suspensions

Cell type	Volume fraction	Number of samples	Recorded Cycles
MBA	0.03	3	2
MBA-*lectin*	0.03	3	2
MDCK	0.05	3	2
MDCK-*sec 13*	0.05	3	2

The measured dielectric spectrum was extracted from the corrected impedance data using an equivalent electric circuit (Fig. 4). Here $C_m = C_0(\varepsilon' - j\varepsilon'')$ is the complex capacitance of the suspension and R_m represents the leakage current through the capacitor (dc conductivity). Extraction of phase parameters was performed by fitting the mixed dielectric equation (Eq. 1) to the measured dielectric spectrum according to the procedure suggested before [33].

3.3. Linearity effect and impedance corrections

The polarization impedance is independent of current densities only for small densities. This phenomenon is critical mainly in high conductive samples and on low frequencies [37]. Here linearity of the impedance was checked for platinum black electrodes (~0.7 cm²), against large reference, in DMEM solution for frequency range from 100 Hz up to 1 kHz (Figs. 5a, b).

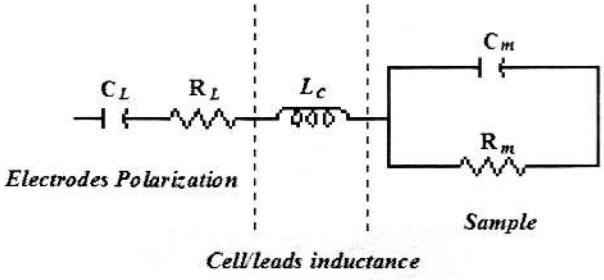

Fig. 4. Equivalent electrical circuit. The sample is represented by parallel capacitor (C_m) and resistor (R_m) which stand for permittivity and conductivity, respectively. The effect of cell/leads inductance and polarization impedance is modeled by inducer (L_c) and resistor-capacitor (R_L, C_L) elements in series with the sample

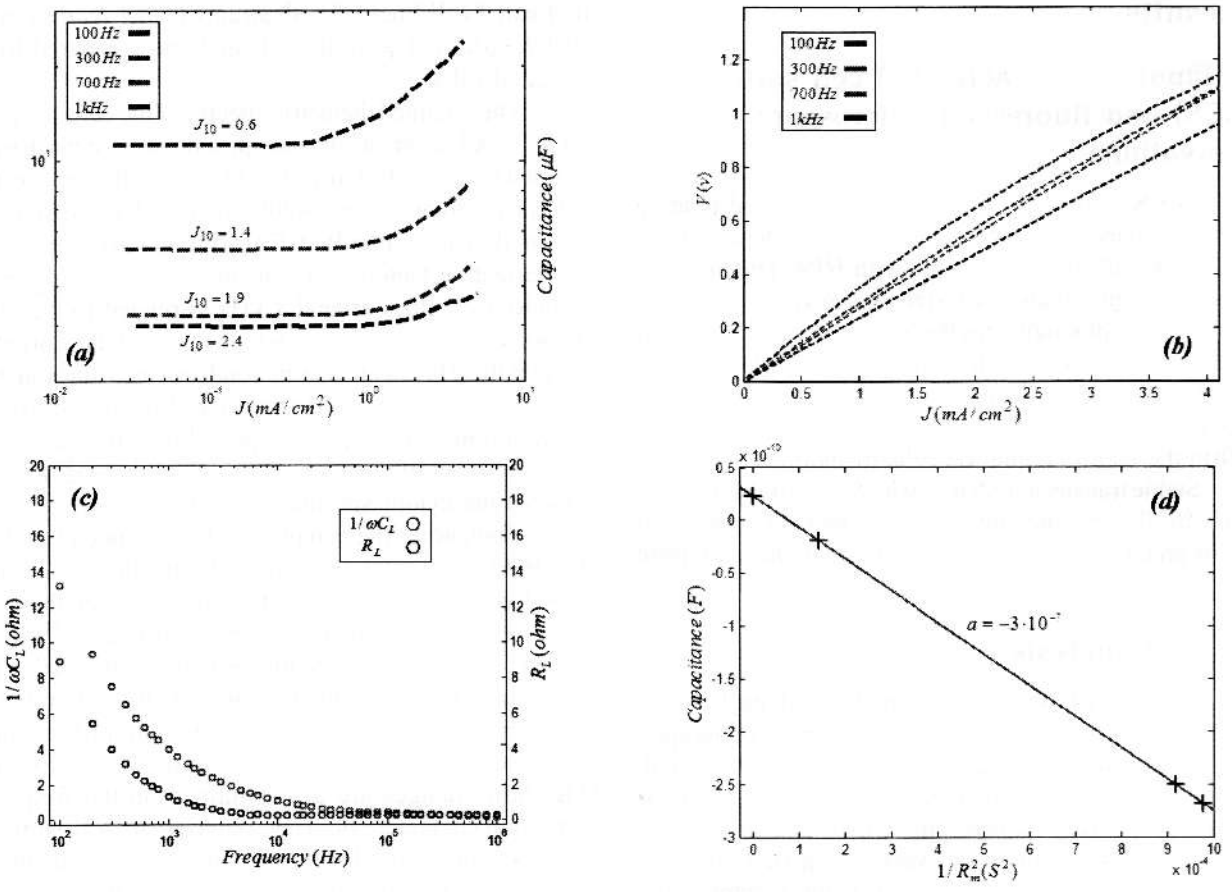

Fig. 5. Pt black electrodes and inductance characteristics.

Voltage versus current density at 100, 300, 700 and 1000 Hz (a): the limit of linearity is continuously increased with frequency. Polarization capacitance versus current density at 100, 300, 700 and 1000 Hz (b): J_{10} indicates the current density at 10 % deviation from linearity. Effect of polarization impedance as function of frequency (c): the impedance exponentially fades as the frequency increases. Apparent capacitance as function of medium resistivity (d): the inductance is extracted by the slope of the obtained curve. The measurements were performed at high frequency (1MHz) to avoid the electrodes polarization effect

The results indicate the limit density of 0.6 mA/cm² at low frequencies, up to 2.4 mA/cm² at 1 kHz. It means that the limit of linearity shifts towards higher current densities as the frequency is increased. Based on those results, the voltage of linearity should be set for <200 mV in order to avoid non-linear effects which introduce significant errors to the impedance signal.

Electrode polarization was corrected for both resistance and capacitance effects (Fig. 5c) based on the procedure suggested before [38]. Here polarization capacitance (C_L) and resistance (R_L) are given by:

$$\frac{1}{C\omega}=\left(1+\frac{1}{(RC\omega)^2}\right)\cdot\left(\frac{1}{C_L\omega}+\frac{R_m^2C_m\omega}{(R_mC_m\omega)^2+1}\right) \quad (6)$$

$$R=\left(1+(RC\omega)^2\right)\cdot\left(R_L+\frac{R_m}{1+(R_mC_m\omega)^2}\right) \quad (7)$$

where R_m is the sample resistance, C_m is the sample capacitance; R and C are the measured parameters of the sample. Based on the low volume fraction of cells, the shielding effect caused by the cells is negligible, and therefore, the reliability of this correction technique is high [39].

Inductance of leads/capacitor was evaluated at high frequency (1MHz) when the measured impedance is free from polarization effects (Fig. 5d) [40]. Here the sample capacitance was measured as a function of sample conductivity (electrolyte concentration). The inductance is then calculated as the slope of the obtained curve, when

$$L_c=-\frac{dC_m}{dR_m^{-2}} \quad (8)$$

4. Results

4.1. Fluorescence-activated cell sorter (FACS) and fluorescent microscopy observations

FACS analysis of *MBA-15* cells revealed binding of *HPA* to cell membrane. Histogram (Fig. 3a) demonstrates 85 % of the cells that are stained with *HPA*. The intensity of cell staining versus cells size is shown by dot plots (Fig. 3b). This plot indicates the homogeneity of the tested suspension based on the forward scatter (FSC) of each cell. The obtained results indicate that the tagged suspension (*HPA+*) is homogenous, and therefore, confirm the *lectin* tagging on cells membrane.

Stable transfected *MDCK* with *SEC13*-GFP are seen clearly by fluorescence microscope. The over expressing cells of green protein is distributed through the cytoplasm (Fig. 3c).

4.2. AFM analysis

The morphological parameters of cells were measured using Atomic Force Microscopy. Topography (Fig. 1) of both *MBA* and *MDCK* cells was recorded. Several cells were then analyzed in order to obtain their average geometrical dimensions. Cross-section analysis revealed information about the average dimensions of *MBA* and *MDCK* cells respectively: Average length (central axis): 24 μm, 26 μm; Average width (central axis): 10 μm, 18 μm; average height (central axis):1.2 μm, 1.6 μm.

4.3. Dielectric measurements

Based on the topography of *MBA* and *MDCK* cells (Fig. 1), both of them can be approximated as single-shell ellipsoids. Here the cytoplasm is bound by a membrane of finite thickness *d*, with inner dimensions R_{ix}, R_{iy}, R_{iz}. The interface (phospholipids membrane), that separates the different dielectric layers, introduces two possible dispersion mechanisms caused by both conductivity and permittivity differences between the cytoplasm and the exterior medium.

When multiple dispersions exist, each is sensitive to relaxation at a specific interface. Here the interface of the membrane-cytoplasm is expected to be most sensitive to the changes related to conductivity and capacitance of these components (*Maxwell-Wagner* effect). It means that the induced dipole, and hence the complex dielectric spectrum, are dependent on the electrical properties of both membrane and cytoplasm.

Due to the dielectric properties of cells, the cytoplasm conductivity and the membrane permittivity should be influenced by molecular changes occurring on those phases respectively. Here *MBA* and *MDCK* cell lines have been subjected to dielectric spectroscopy. In addition, the treated cell lines of both strains (*MBA-lectin* coated, *MDCK- SEC13*) were investigated and compared to the untreated cells.

The obtained dielectric spectra of the cells are given in Fig. 6. All experiments indicate a dispersion mechanism which is accounted for the *Maxwell-Wagner* effect (interfacial polarization). Additionally, sub dispersions are obtained, which resulted from large variation of the depolarization factors along the three axes. The deviation of dielectric values around 1 kHz is related to the effect of electrode polarization, which can not be corrected completely. The steep rise in conductivity values at high frequencies is related to contribution of additional dispersion mechanism, which probably is related to pure dielectric relaxation governed by permittivity differences between the cytoplasm and the medium.

Comparing the complex dielectric spectra of *MBA WT* (*Wild Type*, untreated cells) cells and the *lectin* coated cells (Fig. 6a) reveals clear differences between those two cell lines. The obtained dielectric constant (ε') of the treated cells is found to be higher than the *WT* cells. This rise is expected due to the presence of charged groups on the membrane, which affect its capacitive part. Additionally, based on the dielectric loss (ε'') spectrum (Fig. 6d), changes are also obtained on the frequency dispersion characteristic. Here the loss factor is shifted to lower frequencies due to the increase of membrane capacitance. This is caused by the change in polarization relaxation time of cells: $f_{mem-cyt} = 1/\tau_{mem-cyt}$, which is affected from both membrane capacitance and cytoplasm conductivity ($\tau_{mem-cyt}$ increased).

The obtained *MDCK* spectra (Figs. 6b, c), demonstrate remarkable differences at relatively high frequencies when charge and ion migration (conductive polarization) start to fade. This happens when the frequency exceeds the inverse relaxation time ($\tau_{med-mem}$) of the medium-membrane interface. Here the *SEC13* cells exhibit higher dispersion characteristics comparing to the *WT* cells. This is probably caused by the changes occurred in cytoplasm conductivity, which affected the cytoplasm-membrane relaxation time. The characteristic frequency of cells ($\tau_{mem-cyt}$) is now increasing due to the decrease in cytoplasm resistivity.

In order to estimate the exact dielectric parameters of the cells, the mixed dielectric equation (Eq. 1) was fitted to the experimental data. Here the best phase parameters have been evaluated based on the average values of 6 measurements for each cell type. Additionally, the membrane conductivity, which is very low, especially in non-excitable cells [41], was neglected and assumed to have no effect on the obtained spectra. The thickness of *MDCK* and *MBA* membranes was taken to be 6 nm [42-47]. The fitted parameters are summarized in Table 2.

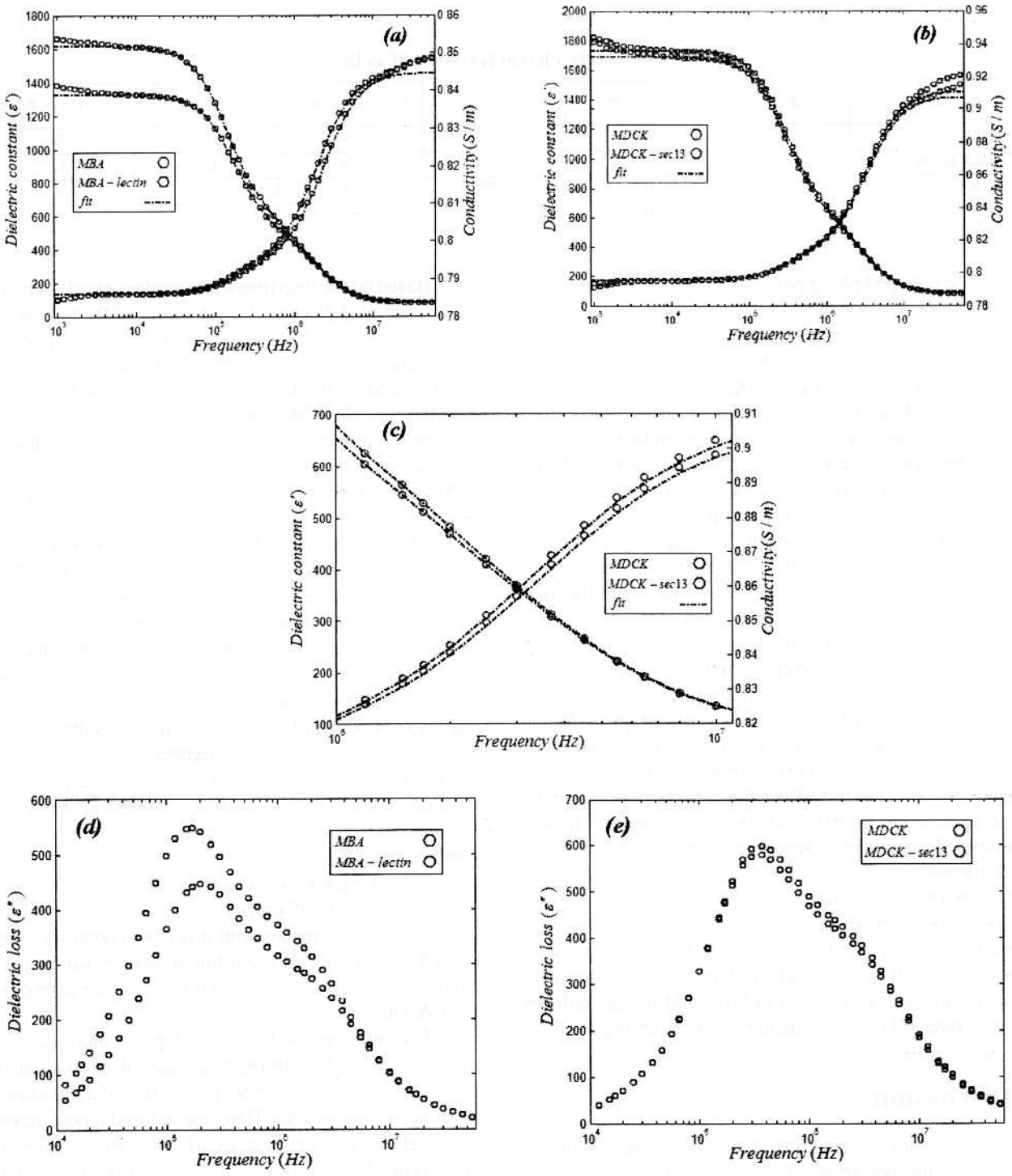

Fig. 6. Dielectric spectra of *MBA* and *MDCK* cell suspensions: dielectric and conductivity spectra of *MBA* and *MBA-lectin* suspensions (a), dielectric and conductivity spectra of *MDCK* and *MDCK-sec13* suspensions (b), high frequency observation on *MDCK* and *MDCK-sec13* spectra (c), loss spectra of *MBA* and *MBA-lectin* suspensions (d), loss spectra of *MDCK* and *MDCK-sec13* suspensions (e)

Table 2

Dielectric characteristics of cells

Cell	ε_m	$\sigma_m(mS/cm)$	ε_{om}	$C_{mem}(\mu F/cm^2)$	ε_i	$\sigma_i(mS/cm)$
MBA	81	8.5	6.11	0.54	68	7.24
MBA-*lectin*	81	8.5	7.53	0.66	67	7.12
MDCK	84	9.1	4.72	0.42	70	9.30
MDCK-*sec 13*	84	9.1	4.85	0.43	73	9.98

The obtained phase parameters indeed indicate clear changes between both *WT* cell lines and their mutants. As expected, the membrane capacitance of *lectin* tagged *MBA* cells was found to be higher than in the *WT* cells. In addition, small changes in cytoplasm conductivity and permittivity are noticed; those may be related to sub structural or molecular changes caused by the *lectin* binding.

The phase parameters of *MDCK* cell lines indicate clear difference in cytoplasm conductivity between *WT* and treated cell lines. This change is related to the over-expression of *SEC13* protein. The small change in cytoplasm permittivity may be attributed to the polarization characteristics of this protein which is additive to the total dielectric polarization (ε'_{cyt}) of the cytoplasm.

The effect of membrane conductivity was evaluated separately in order to avoid errors in the fitted parameters. Phase parameters were found to be independent of membrane conductivity up to values of $\sim 10^{-5}$ S/m. When membrane conductivity was increased, major changes were obtained on membrane permittivity (ε_{om}). Those changes however, didn't affect the ratio between parallel phase parameters of *WT*, and treated cell lines, on both cell types. It means that membrane conductivity can only fundamentally affect membrane permittivity. If the conductivity is low (low ion channels activity), then it behaves like a pure dielectric membrane with large capacitance values. Otherwise, when the conductivity is significant (high ion channels activity), the membrane is partially lumped with the cytoplasm and hence, reduces the effective influence of membrane as isolating shell.

5. Discussion

This study is aiming to demonstrate the use of DS as a screening tool after cellular and molecular markers. The screening ability of fine differences on membrane permittivity, and cytoplasm conductivity, has been demonstrated using *MBA* and *MDCK* cells respectively. The analysis is based on the comparison of differences in intra-cellular proteins using *MDCK* over-expressing *SEC13* and membrane binding of *lectin* on cell surface of *MBA* cells. The observed dielectric spectra allow clear distinction between treated and untreated cell lines and hence, confirm the applied biological modification on both treated cell lines.

Based on the fitted phase parameters of cells, changes in the matching dielectric characteristics of the tagged cells were observed (Table 2). Those changes are well adapted to the cellular and molecular state of modified cells. The *lectin* coating on *MBA* cells increased membrane permittivity. Here the membrane is more polar and hydrophilic comparing to the membrane of the untreated cells. The obtained relative permittivity values (*MBA-lectin*= = 7.53, *MBA* = 6.11) are therefore representative of those changes.

The cytoplasm conductivity of *MDCK-SEC13* cells was clearly affected by the over-expression of *SEC13* protein. *SEC13* is known to be one of the most important proteins related to transport mechanism between the ER (Endoplasmic Reticulum) and Golgi apparatus; Its main activity is related to vesicles budding and release [48, 49]. In cytoplasm, *SEC13* is found as part of heterooligomery complex (150 kDa) [49]. Based on its molecular function it seems reasonable that over-expression of *SEC13* will lead to additional sub-expressions and formation of associate proteins related to this complex. Therefore, the net molecular charge in cytoplasm will also be affected by those products.

The obtained cytoplasm conductivity of *MDCK-SEC13* cells (9.98 mS/cm) is therefore partially affected by the above phenomenon, but it is not in contradiction to the fundamental finding regarding more general change in cytoplasm conductivity when compared to the native cells (9.3 mS/cm).

The obtained differences in phase parameters of cells can be clarified through the use of equivalent two phase model, which describe the nature of relaxation in single shell ellipsoid cells. Here, the induced dipole depends on the electrical properties of both membrane and cytoplasm. Therefore, the internal interface of the membrane and hence the membrane-cytoplasm relaxation time, should be affected by the molecular changes occurring on those two phases.

At a low frequency the conductive polarization is dominant over dielectric polarization; therefore, the conductive charging of membrane is producing large polarization across the membrane. When the frequency is increased so that it exceeds the inverse *RC* time of the polarized membrane-cytoplasm interface, field penetration

into the cytoplasm interior will occur, resulting in dispersion (relaxation) that is governed by the conductivity of the cytoplasm and membrane capacitance.

The equivalent electric circuit of the above phenomena is modeled by two parallel *R-C* (resistor-capacitor) elements [50-52] which represent the conductivity and capacitance of both membrane and cytoplasm. The relaxation time of the equivalent system is given by Equation 9.

$$\tau = \frac{R_{cyt} R_{mem} \left(C_{cyt} + C_{mem}\right)}{R_{cyt} + R_{mem}} \tag{9}$$

The thin dielectric membrane capacitance is given $\varepsilon_{mem} / d_{mem}$ by when $d_{mem} << d_{cyt}$, therefore, it is much higher than that of the cell interior. Since membrane of biological cells is considered as low conductivity elements [41], the resistor component (R_{mem}) can be neglected (yields very high resistivity). The low conductive membrane is then assumed to be an ideal insulating membrane. Therefore, the charge relaxation time is simple resistor-capacitor relaxation time, when the membrane capacitor is coupled to the conductive cytoplasm (resistor).

$$\tau = R_{cyt} C_{mem}, \sigma_{mem} = 1/R_{mem} \to 0$$
$$C_{mem} >> C_{cyt} \tag{10}$$

In order to define the relaxation time in ellipsoid cell systems, the permittivity equation for shelled-ellipsoid cell (Eq. 2) can be modified to Debye type (Eq. 11) [53-55]. It should be assumed that both of the components (membrane and cytoplasm) are loss free, and also have well defined constant characteristics at the given frequency range. This assumption does not exclude the possibility that those components demonstrate dielectric loss in higher frequency range.

$$\bar{\varepsilon}_{ck} = \varepsilon_{hk} + \frac{\varepsilon_{lk} - \varepsilon_{hk}}{1 + j\omega\tau_k} + \frac{\tilde{\sigma}_k}{j\omega\varepsilon_0}, \; k = x, y, z \tag{11}$$

Here ε_{hk} is the limit is the limit of permittivity at high frequency, is the dispersion magnitude, is the relaxation time, is the angular frequency and is the dc conductivity at low frequencies. Based on Eqs. 11 and 2, the relaxation time across each axes of the ellipsoid is given by:

$$\tau_k = \varepsilon_0 \frac{\varepsilon'_{om} + \left(L_{ik} - vL_k\right)\left(\varepsilon'_i - \varepsilon'_{om}\right)}{\sigma_{om} + \left(L_{ik} - vL_k\right)\left(\sigma_i - \sigma_{om}\right)} \tag{12}$$

For low conducting and very thin membrane the relaxation time is rewritten as:

$$\tau_k = \varepsilon_0 \frac{\varepsilon'_{om}}{\sigma_i \left(L_{ik} - vL_k\right)}, \; \sigma_{om} \to 0,$$
$$\left(L_{ik} - vL_k\right) \to 0 \tag{13}$$

The relaxation times and characteristic frequencies of both native and treated *MBA* and *MDCK* cell lines are summarized in Table 3. In addition, the dielectric loss spectra of cells are given in Fig. 7.

Table 3

Relaxation and frequency characteristics

Cell	$\tau_x(s)$	$f_x(MHz)$	$\tau_y(s)$	$f_y(MHz)$	$\tau_z(s)$	$f_z(MHz)$
MBA	$8.9 \cdot 10^{-7}$	1.1	$1.5 \cdot 10^{-7}$	6.7	$1.3 \cdot 10^{-8}$	76.9
MBA-*lectin*	$1.1 \cdot 10^{-6}$	0.9	$2.9 \cdot 10^{-7}$	3.4	$1.7 \cdot 10^{-8}$	58.8
MDCK	$5.3 \cdot 10^{-7}$	1.9	$9.4 \cdot 10^{-8}$	10.6	$8.2 \cdot 10^{-9}$	121
MDCK-*sec 13*	$5.1 \cdot 10^{-7}$	2.0	$8.9 \cdot 10^{-8}$	11.2	$7.9 \cdot 10^{-9}$	126

As suggested in the result section, both cell lines exhibit differences in relaxation times between *WT* and mutants (treated cells). Both differences are attributed to changes occurred on cytoplasm conductivity and membrane permittivity which affected the conductive relaxation of the cells. The increase of relaxation times in *MBA-lectin* tagged cells is attributed to the rise of membrane permittivity. Here the charging effect caused by *lectin* antibodies, increased the membrane capacitance, and hence, increased the relaxation times of the cells. The opposite effect is observed in *MDCK* cell lines. Here the over-expression of *SEC13* protein increased the cytoplasm conductivity (resistivity decreased) and hence, the relaxation times were found to be lower than expected. The equivalent loss plots (Fig. 7) support those findings. Here the characteristic frequencies found to be slightly shifted according to the changes occurred in relaxation times of both cells.

Those changes are directly attributed to the differences occurred in dielectric characteristics of the treated cells (*MBA-lectin, MDCK- SEC13*) comparing to the native ones. Of course, changes on relaxation times of cells lead to changes on relaxation times of the whole cells-medium system, and therefore, differences are also obtained in the dielectric spectra as presented in Figs. 6d and e.

The unique findings presented in this study highlight the power of dielectric spectroscopy as a potential screening tool after molecular and cellular markers. Here, target identification of specific cellular phenotypes has been demonstrated using dielectric screening method. Using the fundamentals of mixed dielectric theories, the electric properties of cells were determined by fitting the well-established shelled-ellipsoid model into the measured spectra. Those unique properties were found to be well adapted to the molecular and structural state of the analyzed cells.

The high sensitivity of DS, as demonstrated here as well as by other authors [6-9, 21-25, 56-61], has a promising potential as a screening tool on live cell libraries. It can be used for quantative and systematic analysis on multiple Micro-libraries labeled with specific probes in non invasive and non destructive way. It can also allow real time screening after fine biochemical effects on both cellular and molecular level, which can not be detected using the traditional screening assays.

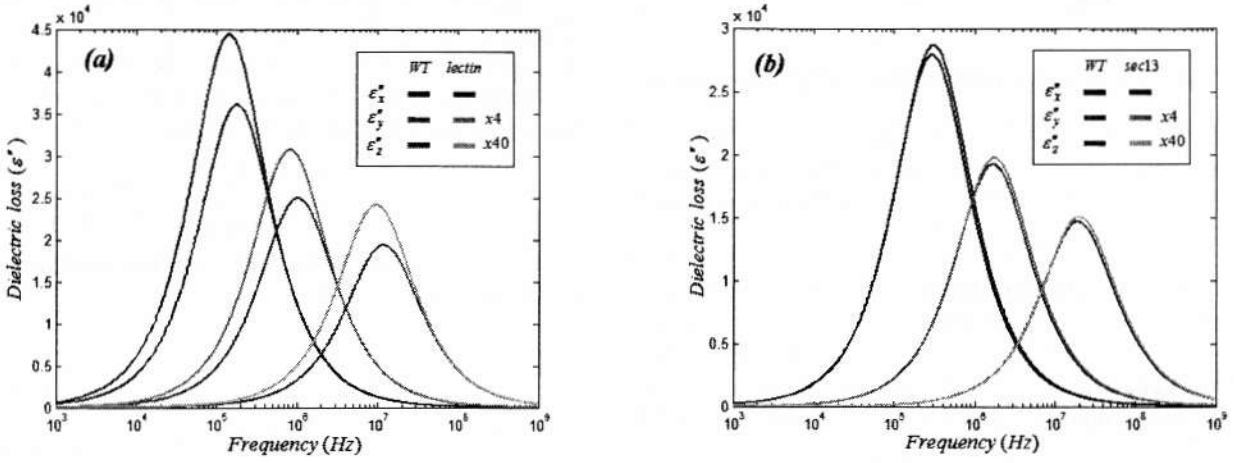

Fig. 7. Loss spectra of *MBA* and *MDCK* cells: *MBA* and *MBA-lectin* cells (a), *MDCK* and *MDCK-sec13* cells (b). Here the losses are given by the *x, y, z* axes of cells

List of symbols

R_{ix}, R_{iy}, R_{iz} - Semi axes of cell.

Δ_L - Thickness of phospholipids membrane.

N - Number of cells.

Φ - Volume fraction of cells.

ε_m^* - Complex permittivity of external medium, when:

$$\varepsilon_m^* = \varepsilon_m' - j\varepsilon_m'' = \varepsilon_m' - j\sigma_m/(\omega\varepsilon_0).$$

ε_{om}^* - Complex permittivity of membrane, when:

$$\varepsilon_{om}^* = \varepsilon_{om}' - j\varepsilon_{om}'' = \varepsilon_{om}' - j\sigma_{om}/(\omega\varepsilon_0).$$

ε_i^* - Complex permittivity of cytoplasm, when:

$$\varepsilon_i^* = \varepsilon_i' - j\varepsilon_i'' = \varepsilon_i' - j\sigma_i/(\omega\varepsilon_0).$$

ε_0 - Permittivity of free space $= 8.85 \cdot 10^{-12}\, C^2/Nm^2$.

med - External medium.

mem - Membrane.

cyt - Cytoplasm.

d - Thickness.

References

[1] Hoeber R.: Eine Physiol. Anatom. Studie, 1910, **133,** 237.
[2] Schwan H., Bothwell T. and Wiercinski F.: Fed. Proc. Am. Soc. Exp. Biol., 1954, **13,** 15.
[3] Schwan H. and Bothwell T.: Nature, 1956, **178,** 265.
[4] Schwan H. and Carstensen E.: Science, 1957, **125,** 985.
[5] Irimajiri A., Hanai T. and Inoue A.: J. Theor. Biol., 1979, **78,** 251.
[6] Surowice A., Stuchly S. and Izaguirre C.: Phys. Med. Biol., 1986, **31,** 43.
[7] Asami K., Takahashi Y. and Takashima S.: Biochem. Biophys. Acta, 1989, **1010,** 49.
[8] Bordi F., Cametti C., Rosi A. and Calcabrini A.: Biochem. Biophys. Acta, 1993, **1153,** 77.
[9] Beving H., Eriksson L., Davey C. and Kell D.: Eur. Biophys. J., 1994, **23,** 207.
[10] Foster K. and Schwan H.: Dielectric Crit. Rev. Biomed. Eng., 1989, **17,** 25.
[11] Onsager L.: J. Am. Chem. Soc., 1936, **58,** 1482.
[12] Pethig R.: Dielectric and electronic properties of biological materials. John Wiley & Sons Ltd., New York 1979.
[13] Grant E., Sheppard R. and South G.: Dielectric behaviour of biological molecules in solutions. Clarendon Press, Oxford 1978.

[14] Takashima S.: Electrical properties of biopolymers and membranes. Institute of Physics Publishing, Philadelphia 1989.
[15] Haggis G., Buchanan T. and Hasted J.: Nature, 1951, **167,** 607.
[16] Grant E.: Nature, 1962, **196,** 1194.
[17] Keefe S. and Grant E.: Phys. Med. Biol., 1974, **19,** 701.
[18] Gough S.: J. Solution Chem., 1983, **12,** 729.
[19] Mashimo S., Kuwabara S., Yagihara S. and Higashi K.: J. Phys. Chem., 1987, **91,** 6337.
[20] Miura N., Asaka N., Shinyashiki N. and Mashimo S.: Biopolymers, 1994, **34,** 357.
[21] Asami K., Gheorghiu E. and Yonezawa T.: Biochem. Biophys. Acta, 1998, **1381,** 234.
[22] Asami K.: Biochem. Biophys. Acta, 1999, **1472,** 137.
[23] Asami K. and Hanai T.: Colloid Polym. Sci., 1992, **270,** 78.
[24] Irimajiri A., Ando M., Matsuoka R., Ichinowatari T. and Takeuchi S.: Biochim. Biophys. Acta, 1996, **1290,** 207.
[25] Asami K., Gheorghiu E. and Yonezawa T.: Biophys. J., 1999, **76,** 3345.
[26] Raicu V., Saibara T., Enzan H. and Irimajiri A.: Bioelectrochem. Bioenerg., 1998, **47,** 333.
[27] Asami K. and Irimajiri A.: Phys. Med. Biol., 2000, **45,** 3285.
[28] Frick H.: Phys. Rev., 1924, **24,** 575.
[29] Frick H.: J. Appl. Phys., 1953, **24,** 644.
[30] Pauly H. and Schwan H.: Naturforsch Zh., 1959, **14,** 125.
[31] Hanai T., Koizumi N. and Irimajiri A.: Biophys. Struct. Mechanism, 1975, **1,** 285.
[32] Redwood W.R., Takashima S., Schwan H. and Thompson T.: Biochim. Biophys. Acta, 1972, **255,** 557.
[33] Asami K., Hanai T. and Koizumi N.: Jpn. J. Appl. Phys., 1980, **19,** 359.
[34] Benayahu D., Kletter Y., Zipori D. and Wientroub S.: J. Cell Physiol., 1989, **140,** 1.
[35] Shur I., Marom R., Lokiec F., Socher R. and Benayahu D.: J. Cell. Biochem., 2002, **87,** 51.
[36] Shefer G., Carmeli E., Rauner G. *et al.*: J. Cell Physiol., 2007, in press.
[37] Onaral B. and Schwan H.: Med. & Biol. Eng. & Comput., 1982, **20,** 299.
[38] Schwan H.: Biophysik, 1966, **3,** 181.
[39] Schwan H.: Ann. Biomed. Eng., 1992, **20,** 269.
[40] Schwan H.: Phys. Techn. in Biolog. Res., Academic Press, 1963, **VI,** 323.
[41] Johnston D. and Miao-Sin Wu S.: Foundations of cellular neurophysiology. MIT press 1995.
[42] Larmer J., Schneider S.W., Danker T., Schwab A. and Oberleithner H.: Eur. J. Physiol., 1997, **434,** 254.
[43] Bicknese S., Periasamy N., Shohet S. and Verkman A.: Biophys. J., 1993, **65,** 1272.
[44] Garavaglia M. *et al.*: Cell Physiol. Biochem., 2004, **14,** 231.
[45] Elliott J., Tona A., Woodward J., Meuse C., Elgendy H. and Plant A.: IEEE Proc. Nanobiotechnol., 2004, **151,** 75.
[46] Rao N., Plant A., Silin V., Wight S. and Hui S.: Biophys. J., 1997, **73,** 3066.
[47] Rao N., Silin V., Ridge K., Woodward J. and Plant A.: Anal. Biochem., 2002, **307,** 117.
[48] Shaywitz D. *et al.*: J. Cell Biol., 1995, **128,** 769.
[49] Salama N., Yeung T. and Schekman R.: EMBO J., 1993, **12,** 4073.
[50] van Beek L.: Prog. Dielect., 1967, **7,** 69.
[51] Maxwell J.: Electricity and magnetism. Clarendon, Oxford 1892.
[52] Wagner K.: Die Isolierstoffe der elektrotechnik. Springer, Berlin 1924.
[53] Debye P.: Polar molecules. Dover Publications, New York 1929.
[54] Asami K.: Prog. Polym. Sci., 2002, **27,** 1617.
[55] Tuncer E., Serdyuk Y.V. and Gubanski S.: IEEE Trans. Dielect. Electr. Insul., 2002, **9,** 809.
[56] Feldman Y., Ermolina I. and Hayashi Y.: Trans. Dielect. Electr. Insul., 2003, **10,** 728.
[57] Feldman Y., Zuev Y., Polygalov E. and Fedotov V.: Colloid Polym. Sci., 1992, **270,** 768.
[58] Polevaya Y., Ermolina I., Schlesinger M., Ginzburg B.Z. and Feldman Y.: Biochim. Biophys. Acta, 1999, **1419,** 257.
[59] Erimolina I., Polevaya Y. and Feldman Y.: Eur. Biophys. J., 2000, **29,** 141.
[60] Hayashi Y., Livshits L., Caduff A. and Feldman Y.: J. Phys. D: Appl. Phys., 2003, **36,** 369.
[61] Prodan C., Mayo F., Claycomb J. and Miller J.: J. Appl. Phys., 2004, **95,** 3754.

БІОЛОГІЧНИЙ СКРИНІНГ НА ОСНОВІ КЛІТИН ДЛЯ СПЕЦІАЛЬНИХ МЕМБРАННИХ І ЦИТОПЛАЗМАТИЧНИХ МАРКЕРІВ З ВИКОРИСТАННЯМ ДІЕЛЕКТРИЧНОЇ СПЕКТРОСКОПІЇ

Анотація. *Показано відображаючий потенціал діелектричної спектроскопії (ДС) за цитоплазматичними і мембранними маркерами для скринінг-аналізу на основі клітин. Вивчено вплив діелектричної проникності і цитоплазмової провідності з використанням мічених МВА і МДСК ліній клітин відповідно. Порівнянням діелектричних спектрів мічених і природних ліній клітин встановлено чітку різницю між ними. Визначено, що існує різниця в діелектричних властивостях клітин. Підтверджено високороздільну здатність і чутливість ДС стосовно молекулярних і клітинних змін і запропоновано використовувати потенціал ДС як неінвазивний засіб скринінгу в дослідженнях біології клітин.*

Ключові слова: *діелектрична спектроскопія, міжфазна поляризація, клітинний скринінг, SEC13.*